

Gene expression. To merge our gene expression data sets from two different platforms, probe sets that were shared between the two platforms were selected and then used the DWD (Distance Weighted Discrimination) method to normalize data across the two platforms, to reduce batch effects. After this process, data from the two platforms were made comparable and combined together for more statistical power, using methods previously described.¹ PCA analysis on the merged data sets shows that data from the two platforms were mixed and we see that the previous clusters due to batch effects were eliminated. The combined data set was transformed to a GCT format file, and a class label CLS file was also created for this combined data matrix.

Unsupervised hierarchical analysis was used to detect sub-clusters/groups within our sample sets. For this analysis we used Pearson Correlation as the distance measure between samples. Sample data was normalized and centered, pairwise complete-linkage method was used as the clustering method.

Copy number analysis: copy number analysis was performed as described previously², with slight modifications. To complete signal normalization and initial copy number estimate by circular binary segmentation, Affymetrix CNAT4.0 software was first used to summarize raw signal intensities (\log_2 ratio) for each sample using an additional set of 250 germline DNA SNP 6.0 arrays as reference. For each sample, signal intensity distribution of each chromosome arm was generated and visually inspected to identify chromosome arms with diploid copy number. Signal intensities were then scaled so that these diploid regions of the genome have the same

median \log_2 ratio across all samples. Using DNACopy, an R version of the circular binary segmentation algorithm, we inferred copy number-changed chromosome segments based on the normalized signal intensities generated above for each sample. For each segment, DNACopy generated a mean \log_2 ratio of all probes in the segment.

To adjust for percentage of blasts in tumor samples, segmentation results from DNACopy, for each patient, was compared: diagnosis vs. relapse \log_2 ratio of all common segments (those with mean \log_2 ratio > 0.1 or < -0.1 in both samples), with a weighted linear regression model:

\log_2 ratio (relapse) = $\beta \times \log_2$ ratio (diagnosis); weights being the number of SNPs in each segment.

We observed that in all cases, the \log_2 ratios were highly correlated between matched diagnosis and relapse samples and in 51 pairs, β was close to 1, suggesting comparable signal intensity and similar blast percentage at diagnosis and at relapse. However, in 5 pairs, the slopes (β) significantly deviated from identity line. For example, a β of 3 indicated that blast percentage in the diagnosis sample was 1/3 of that in the matched relapse sample. The mean \log_2 ratio of this diagnosis sample was therefore adjusted by multiplying it by β (i.e. 3), while no adjustment was made for the relapse sample of this patient.

Quality control and CNA classification

Regions with adjusted mean \log_2 ratio > 0.3 or < -0.3 and encompassing at least 8 SNPs were defined as copy number gains and losses, respectively.

Additional steps of quality control were implemented as follows:

- 1) Using matched germline sample as reference, we first excluded copy number changes arising from inherited copy number variations. Thus, a gain or loss was considered inherited if copy number change was also detected (by DNACopy) in the corresponding germline samples. Additionally, for each tumor CNA region, we compared the probe signal intensities between the tumor sample and the matched germline sample and ensured the differences were statistically significant ($P < 0.05$, paired Wilcoxon test).
- 2) Each tumor CNA (as defined in step 1) was then classified as diagnosis-specific, relapse-specific, or shared by diagnosis and relapse as follows:

A region was considered to have a diagnosis-specific CNA when i) DNACopy inferred gain/loss in the diagnosis sample but diploid in the matched relapse sample, ii) the

difference in signal intensity distribution was statistically significant between diagnosis and relapse ($P < 0.05$, paired Wilcoxon test), and iii) the difference in signal intensity distribution was not statistically significant between relapse and germline ($P > 0.05$, paired Wilcoxon test).

Similar comparisons were performed to define relapse-specific CNAs.

A tumor CNA was considered to be shared between diagnosis and relapse, when i) DNACopy inferred gain/loss in both diagnosis and relapse samples, or ii) DNACopy inferred gain/loss only in the diagnosis or the relapse sample, but the difference in signal intensities between diagnosis vs. relapse was not statistically significant ($P > 0.05$, paired Wilcoxon test) and the difference in signal intensities between diagnosis vs. germline and between relapse vs. germline were both statistically significant ($P > 0.05$, paired Wilcoxon test). In the current analyses, CNAs showing different degree of amplification/deletion in the diagnosis and relapse samples (e.g. hemizygous deletion at diagnosis but homozygous deletion at relapse) were also classified as “shared”. Also note that by applying such criteria, we assigned some regions as gain/loss even though they were not detected by DNACopy. For example, if a deletion was detected by DNACopy in the relapse sample but not in the diagnosis sample, but the above conditions for “shared CNA” were satisfied, we would then consider this region as copy number loss in the diagnosis sample as well.

3) Final CNA tallies were subjected to manual examination of the signal distribution plots.

Methylation. The Infinium array interrogates 27,578 CpG loci, covering 14,475 consensus coding sequence genes and 110 miRNA promoters. The selected CpG loci are located within 1Kb upstream and 500 bases downstream of transcription start sites. On average, DNA methylation of two CpG loci per gene was measured. The level of methylation at each CpG locus was expressed as a β -value, which is the ratio of fluorescent signal from methylated probe to total locus intensity. The β values were corrected for potential dye bias using Methylni software and filtered based on a detection value > 0.1 . β -values range from 0.1 to one, with one indicating 100% methylation of the site.

To analyze the change in methylation from diagnosis to relapse in individual patients a methylation state transition matrix was created for each CpG (Figure S5) in which a β -value

<0.3 indicated an unmethylated state, 0.3-0.75 a hemimethylated state and >0.75 a fully methylated state. A minimum $\Delta\beta$ value, from diagnosis to relapse, of 0.13 (detectable with 95% confidence)³ was met in order to transition to the next classification module. Hypermethylation was scored if the methylation level moved from a less methylated state to a more methylated state. Conversely, hypomethylation was scored for any gene moving to a lower level of methylation. A change in methylation which did not cross into the next state was not considered a significant change in methylation status.

Methylation primer sequences. Primers sequences for validation listed below.

Primer name	Sequence
CDKN2A_01 for	5'- AGGAAGAGAGTtttagaaaattttaatatagtgaaggt-3'
CDKN2A_01 rev	5'- CAGTAATACGACTCACTATAGGGAGAAGGCTaacraacaataaactaactactaaaccaa-3'
CDKN2A_02 for	5'- AGGAAGAGAGGaatgagtttttagtggttttataatggt-3'
CDKN2A_02 rev	5'- CAGTAATACGACTCACTATAGGGAGAAGGCTaaaactttcaatacaataactccctcaa-3'
CSMD1_01 for	5'- AGGAAGAGAGGagaagggtttagtggtataagaggtgt-3'
CSMD1_01 rev	5'- CAGTAATACGACTCACTATAGGGAGAAGGCTcccctacaaaaacccctcaaatttacta-3'
COL6A2_01 for	5'- AGGAAGAGAGggaattttgtatttttaggtagttgttatt-3'
COL6A2_01 rev	5'- CAGTAATACGACTCACTATAGGGAGAAGGCTaataaaaaaaaaaaaaacccccctacaa-3'
COL6A2_02 for	5'- AGGAAGAGAGgggygggggggggggtttttgt-3'
COL6A2_02 rev	5'- CAGTAATACGACTCACTATAGGGAGAAGGCTercctcctctacaactctctaaaccta-3'
PTPRO_01 for	5'- AGGAAGAGAGagtttgaatgggggtttagtagtagt-3'
PTPRO_01 rev	5'- CAGTAATACGACTCACTATAGGGAGAAGGCTacraactaaaactacaacctcaaaccta-3'
NOTCH4_01 for	5'- AGGAAGAGAGgttttttttagttagggatttttagatttt-3'
NOTCH4_01 rev	5'- CAGTAATACGACTCACTATAGGGAGAAGGCTccttacaattctcatccctaaaaaaaaaaa-3'
TOP1MT_01 for	5'- AGGAAGAGAGgttgatagygtattattaggttatagatatgtt-3'
TOP1MT_01 rev	5'-CAGTAATACGACTCACTATAGGGAGAAGGCTTTATATACTATACTAAACCTCAACACTATAAAA-3'

Primers used for RQ-PCR are as follows:

B₂M (5'-ATGTGTCTGGGTTTCATCCATCC-3' and 5'-AGTCACATGGTTCACACGGCA-3')

BIRC5 (5'-CATCTCTACATTCAAGAACTGG-3 and 5'-GGTTAATTCTTCAAACCTGCTTC-3'),

FOXM1 (5'GGAGGAAATGCCACACTTAGCG-3 AND 5'-TAGGACTTCTTGGGTCTTGGGGTG-3')

Primers from Qiagen

ATIC QT00015526

BUB1B QT00008701

CAD	QT00057603
CCNB2	QT00037947
CDKN2A	QT00089964
CENPM	QT01675121
COL6A2	QT00067039
CSMD1	QT00043169
DHFR	QT01668730
FANCD2	QT00034370
GART	QT00075467
GATA5	QT01673777
IFIT5	QT00035756
IMPA2	QT00058604
KCNH2	QT01003254
LAPTM4B	QT01023876
NOTCH4	QT00065023
OBSL1	QT00099155
PAICS	QT00087458
RAD51AP1	QT00079758
SMEK2	QT01023876
TOP1MT	QT00085400
TYMS	QT00052423
WT1	QT00059003

Figure S1. Histogram of the distribution of concordance between methylation and gene expression

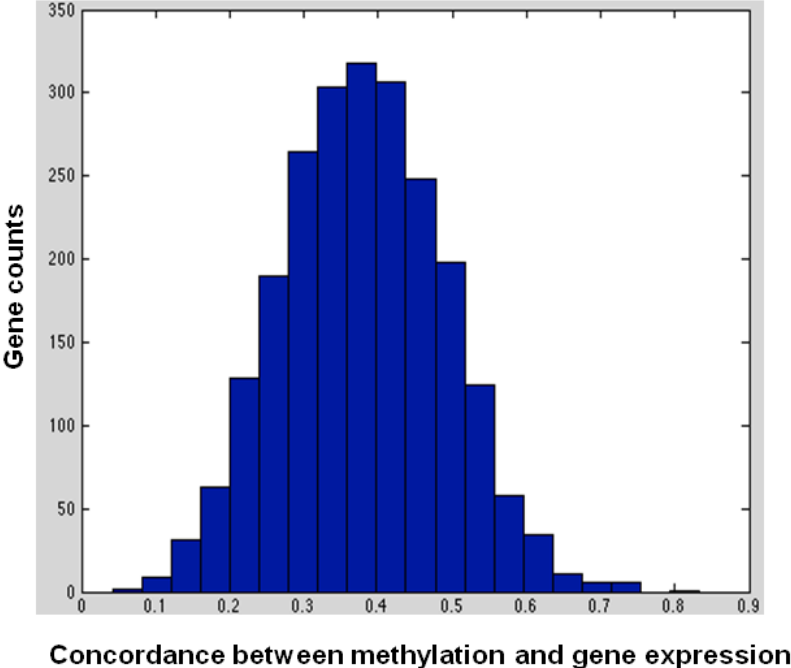


Figure S2. Unsupervised analysis of gene expression data

Cluster analysis where blue dots indicate early relapse samples, those without dots are late relapse samples. Red boxes indicate diagnosis/relapse samples that cluster together.

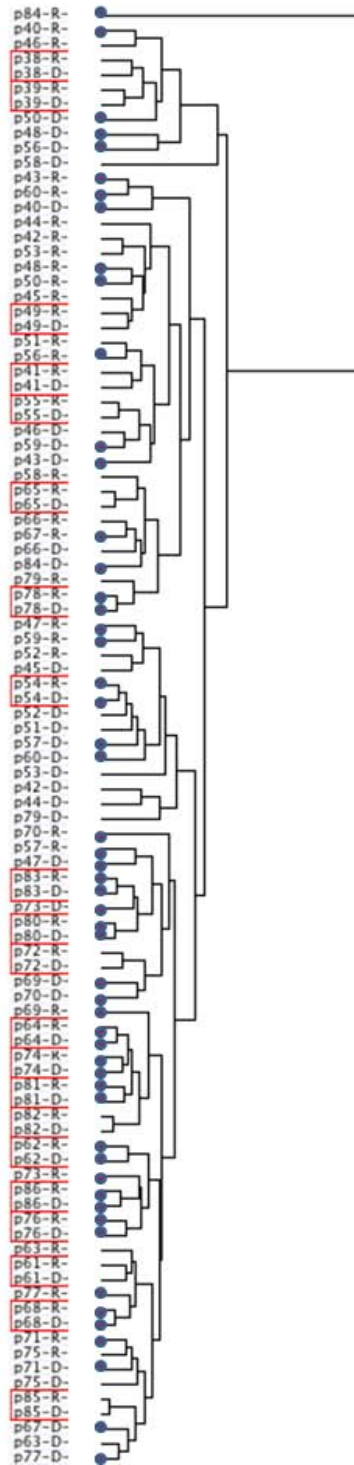


Figure S3. Correlation coefficient of diagnosis/relapse samples versus time to relapse

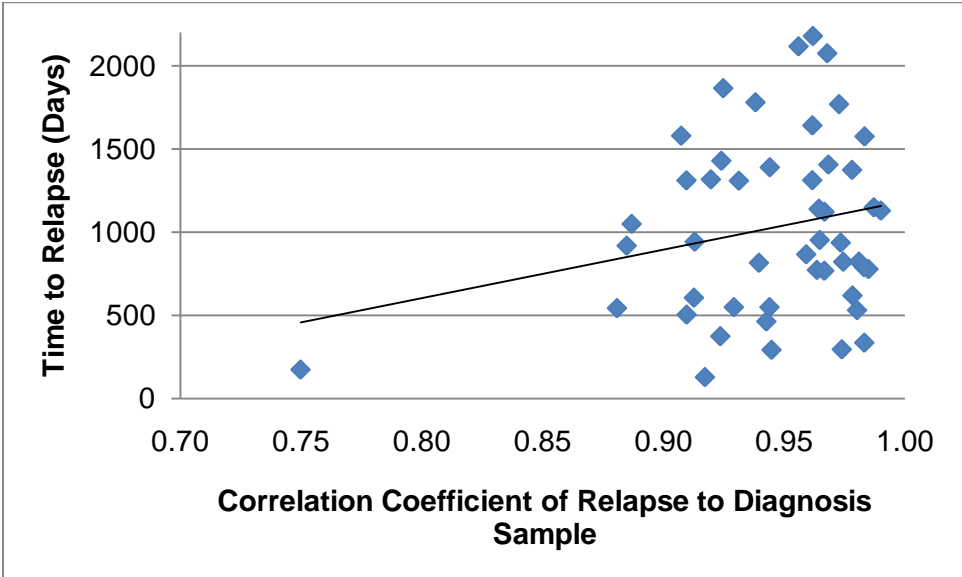


Figure S4. Deletions of MSH6, FBXO11, KCNK12

DNA copy number changes from diagnosis and relapse samples from 56 patients show two deletions specific to relapse at Chr2p16.3. Blue represents deletion.

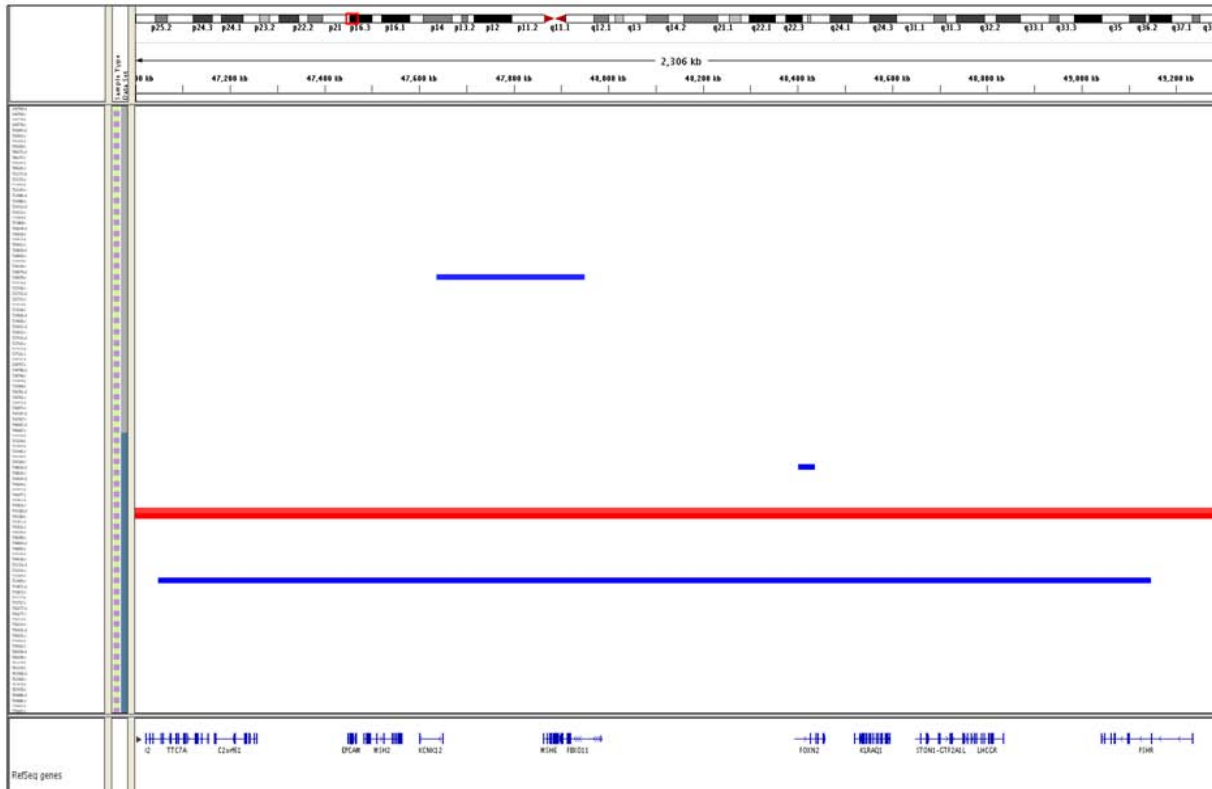
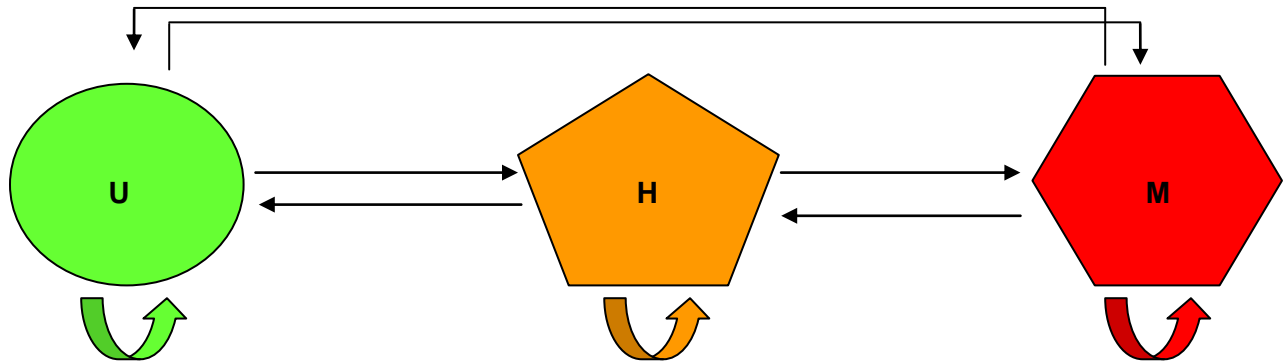


Figure S5. Methylation status transition matrix



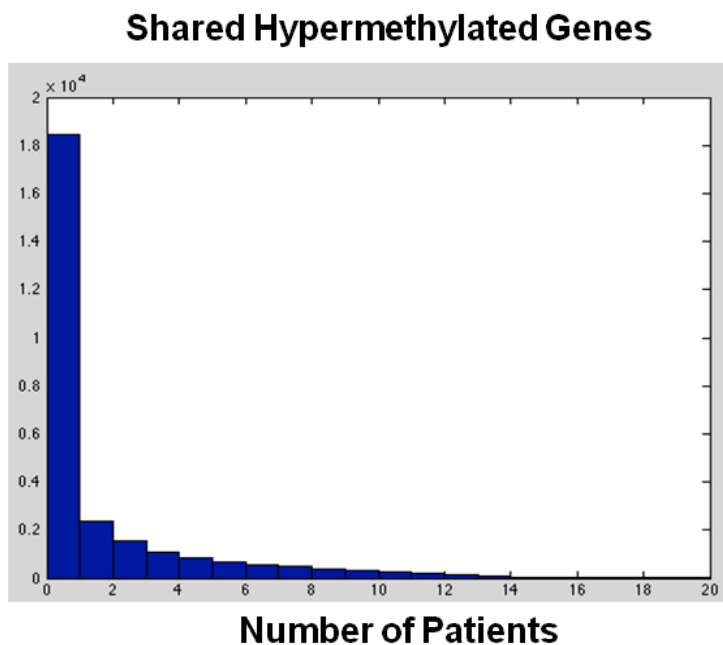
	Unmethylated	Hemi-methylated	Methylated
Unmethylated (U)	UU	UH	UM
Hemi-methylated (H)	HU	HH	HM
Methylated (M)	MU	MH	MM

Hypermethylated

Hypomethylated

Figure S6. Distribution of shared methylated genes

Gene Counts	Patient Counts	Percent
14736	0	1
3699	1	0.465661034
2367	2	0.331532381
1549	3	0.245703097
1058	4	0.189535137
848	5	0.151171223
693	6	0.120422076
571	7	0.09529335
491	8	0.07458844
419	9	0.056784393
296	10	0.041591123
284	11	0.03085793
199	12	0.020559867
144	13	0.01334397
114	14	0.008122416
47	15	0.003988687
36	16	0.00228443
13	17	0.000979041
8	18	0.000507651
4	19	0.000217565
2	20	7.25216E-05



Gene Counts	Patient Counts	Percent
15370	0	1
4055	1	0.442671695
2788	2	0.295634201
1990	3	0.194539125
1284	4	0.122380158
825	5	0.075821307
501	6	0.045906157
328	7	0.027739503
225	8	0.015845964
131	9	0.007687287
32	10	0.002937124
29	11	0.001776779
11	12	0.000725216
2	13	0.000326347
4	14	0.000253826
2	15	0.000108782
0	16	3.62608E-05
1	17	3.62608E-05

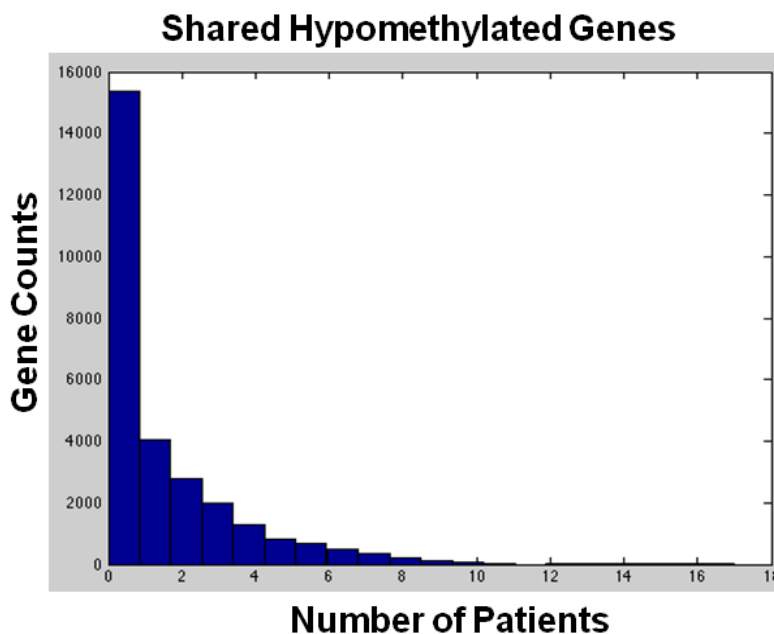


Figure S7. SEQUENOM validation

Validation using SEQUENOM assay was completed in patients that showed significant change in methylation status. Percentage of validation out of total are as follows: *PTPRO*: CpG1 87%, CpG2 79%, *COL6A2*: CpG1 66%, CpG2 66%, CpG3 75%, CpG4 85%, CpG5 82%, *CDKN2A* CpG1 70%, *NOTCH4* CpG1 73%. Validation was unsuccessful for *CSMD1* (CpG1 20%), however the SEQUENOM assay was not optimal for this gene.

